Analytical study of ionizing blast waves in atomic hydrogen

A. Gintrand, S. Bouquet, Claire Michaut

Analytical study of ionizing blast waves in atomic hydrogen

A. Gintrand,[1,2,3] S. Bouquet,[1,2,4] and C. Michaut[2,5]
[1)] *CEA, DAM, DIF, F-91297, Arpajon, France*
[2)] *Laboratoire Univers et THéories (LUTH), Observatoire de Paris, PSL Research University, CNRS, Université Paris Diderot, Sorbonne Paris Cité, F-92190 Meudon, France*
[3)] *Extreme Light Infrastructure ERIC, ELI Beamlines Facility, Za Radnici 835, 252 41 Dolní Břežany, Czech Republic*
[4)] *Université Paris-Saclay, CEA, Laboratoire Matière en Conditions Extrêmes (LMCE), F-91680 Bruyères-le-Châtel, France*
[5)] *Université Côte d'Azur, Observatoire de la Côte d'Azur, CNRS, Laboratoire Lagrange, Campus Valrose, F-06108 Nice Cedex 2, France*

(*Electronic mail: antoine.gintrand@gmail.com)

(Dated: 4 December 2023)

The ionization effect on both the evolution and internal structure of a blast wave (BW) is determined in laboratory conditions. In a first step, the Rankine-Hugoniot equations describing the structure of the shock front together with the Saha equation modeling ionization are solved analytically in a consistent way for the conditions of a cold initial atomic hydrogen gas. In a second step, a simplified approach is used by introducing an effective adiabatic index γ^* that takes into account ionization arising at the shock front. Finally, γ^* is used as input data in the self-similar model derived formerly by Barenblatt to describe the structure and the dynamics of the ionizing BW. For the typical laboratory conditions of blast wave experiments, ionization achieves a hydrogen gas compression up to about 11 times at the shock front of the blast wave where a thin and dense shell forms. For such a compression, the value of the effective adiabatic index is $\gamma^* \simeq 1.2$ leading to a self-similar evolution of the BW where its radius $R(t)$ varies according to $R(t) \propto t^{\alpha^*}$ with $\alpha^* \simeq 0.33$. This value of α^* is lower than the adiabatic expansion stage $\alpha = 2/5$ where the total energy of the BW is conserved. Thus, ionization is found to act as a cooling effect at the shock front where a fraction of kinetic energy is absorbed to ionize the gas.

I. INTRODUCTION

A blast wave (BW) results from the release of a huge amount of energy in a small volume. Its study has been of great interest from the expansion of a supernova remnant (SNR) in the interstellar medium (ISM) to the experiments of Z-pinch and laser-induced shocks in the laboratory. During its time evolution, a BW experiences several stages with various expansion rates α with $R(t) \propto t^{\alpha}$ where t is the time and $R(t)$ is the radius of the BW. Three main stages have been identified and have been the subject of numerous publications from the early 40's until now. The most famous one is the Sedov – Taylor stage evidenced theoretically by Taylor [1,2], von Neumann [3], von Neumann and Taub [4] and Sedov[5,6], independently. This regime takes place soon after the short ballistic phase ($R(t) \propto t$) and the expansion rate is $\alpha = 2/5$. This value comes out from the assumption of an adiabatic expansion, *i.e.* the energy lost by the BW is supposed to be negligible compared to the initial energy released by the explosion. Two more solutions are of great importance. In opposition to the Sedov – Taylor (ST) solution, they take place in the radiative regime of the BW, *i.e.* when the energy lost by radiation (cooling) becomes a significant fraction of the initial energy. Due to this cooling, the mass density at the BW front becomes very large compared to the mass density of the ambient gas in which the BW propagates and, as a consequence, the BW can be considered as formed of an outer dense and thin shell enclosing a very low-density bubble with uniform pressure $P_B(t)$ – notice that since the thickness of the shell is very small compared to its radius, $R(t)$ represents both the radius of the bubble and the radius of the shell. This situation has been studied extensively for the radiative stage of a SNR. The first solution is the so-called pressure-driven snowplow (PDS) solution[7–9] that corresponds to an adiabatically expanding bubble, $P_B(t)R(t)^{3\gamma} =$ constant where γ is the adiabatic index of the gas, pushing the shell with the pressure $P_B(t)$. Since, on the other hand, $P_B(t) \propto (dR/dt)^2$, we conclude that the radius obeys the law $R(t) \propto t^{\alpha_{PDS}}$ where $\alpha_{PDS} = 2/(2+3\gamma)$ and where $\alpha_{PDS} = 2/7$ for $\gamma = 5/3$. As expected, the expansion is slower than for the ST solution because of the energy losses at the surface of the BW. The second solution is the solution by Oort[8,10,11] also known as the momentum-conserving snowplow (MCS) solution. In this stage, the pressure $P_B(t)$ drops to zero due to some cooling effects in the bubble (like radiation), and the shell is not pushed anymore by the inner bubble. Therefore the momentum of the shell is preserved and it can be shown that $R(t) \propto t^{\alpha_{MCS}}$ where $\alpha_{MCS} = 1/4$. The expansion of the BW is much more decelerated than for the PDS solution and α_{MCS} is the smallest value of the expansion rate that can be achieved. However, this asymptotic regime has not been observed during the simulation of SNR[9,12] and may not be able to occur before the SNR merges with the ISM. The radiative stage of the BW has also been demonstrated in the laboratory using z-pinch machines[13–15] and high energy lasers[16–20]. In the experiments by Grun *et al.* [16], Riley *et al.* [20], Edens *et al.* [21], the comparison between the propagation of a BW in nitrogen and in xenon ambient gas is made to demonstrate the effect of radiation cooling on the evolution and stability of the BW. Indeed the BW in nitrogen is found to be non-radiative and stable with an adiabatic expansion rate

$\alpha \approx 2/5$. In the xenon gas, strong radiation emissions are measured and the BW becomes unstable with a lower expansion rate $\alpha < 2/5$. Also, the radiative shock is found to compress up to 35 times the ambient xenon gas in the experiment by Reighard *et al.* [22].

Apart from radiative cooling, other phenomena like phase transitions, dissociation of molecules, or ionization (of molecules and atoms) arising at the shock front also alter the value of the expansion rate with $\alpha < 2/5$. The physical reason for such a deceleration comes out from the energy absorption for these phenomena to happen. Indeed, the absorbed energy is not anymore available to heat matter behind the BW front and this process can be interpreted as a cooling taking place at the shock discontinuity (see further). In this paper, we study the special case of ionization that takes place at the shock front of a BW. Indeed, for a BW propagating in a gas of atomic hydrogen, the atoms are heated at the BW front and they get ionized. Two main questions can be raised: *i)* How significant is the density compression C (or density contrast) at the shock front due to ionization (potential formation of a dense shell which is a key issue in BW evolution)? and *ii)* How much the expansion of the BW is decelerated? Although ionization at shock fronts has been widely investigated, the connection between C and α in BW has been poorly studied in the literature. In a paper dated 1946, Sachs [23] derived properties of strong shocks where the radiation pressure plays a role. In this regime, hydrogen is fully ionized and because of photons, the maximum density contrast is $C = 7$ irrespectively of the atomic density n_H. This maximum value has been recovered by Michaut *et al.* [24] for hypersonic shock waves. They also examined shocks at lower Mach numbers (the radiation pressure becomes small compared to the thermal one) and they found a density peak with $C \approx 10$ for $n_H \approx 3 \times 10^{20}$ cm^{-3}. It appears therefore that when the importance of radiation decreases, ionization has the upper hand over photons and the gas is more compressed. In the series of articles by Whitney and Skalafuris [25] and by Skalafuris [26,27,28], the authors investigated the propagation of a shock in atomic hydrogen. By considering both ionization and cooling effects, the structure of the shock is analyzed for initial conditions of densities, temperatures, and shock velocities relevant to stellar atmospheres. The compression is found to reach $C \approx 12$ in the internal relaxation region (only ionization) and $C \approx 45$ in the radiative relaxation region (ionization plus radiation) behind the shock front. Another approach has been performed by Nieuwenhuijzen *et al.* [29], also in the context of stellar atmospheres. For $n_H \approx 10^{12}$ cm^{-3} and removing radiation contributions, the authors show that the logarithmic derivative of pressure P w.r.t density ρ, $(d\ lnP/d\ ln\rho)_{ad}$, drops as low as 1.1 during the ionization process, evidencing high compressibility (actually, they get $C \approx 3.5$ although the Mach number M is as small as $M = 2$ – we will consider in the further sections BW with $M \gg 1$) of the gas under a mechanical process like the one produced by the passage of a shock wave. The ratio of the specific heats C_P/C_V for a gas undergoing ionization (notice that C_P/C_V differs from $(d\ lnP/d\ ln\rho)_{ad}$) has been plotted a few years ago in a paper by Robinson and Pasley [30] for $n_H \approx 2 \times 10^{19}$ cm^{-3}. They have obtained $C_P/C_V \equiv \gamma_{heat} \approx 1.36$ during ionization and $C \approx 8$ which is larger than the classical value $(\gamma_{heat}+1)/(\gamma_{heat}-1) \approx 6.5$ for strong shocks. More recently, the structure of a shock wave in fully ionized plasmas, including hydrogen plasma (as the authors work with dimensionless quantities, the value of n_H is not provided), has been considered by Domínguez-Vázquez and Fernandez-Feria [31]. They have shown that a transition region occurs between the steady upstream and downstream flows. However, as the authors restrict themselves to $1 < M < 1.5$, the transposition of this result to a high Mach number BW is uncertain. This question is going to be studied in a dedicated section of our article.

In our work, we are going to derive analytically the value of C produced by ionization and make a direct relationship between C and the associated expansion rate α. For that purpose, we are going to use a former model developed by Sedov [6] and by Barenblatt [32] accounting for cooling at the shock front and leading to the value of α. These authors derived self-similar solutions (SSS) where the expansion rate α is computed numerically from an eigenvalue problem and has a non-analytic dependence on both the adiabatic index of the ideal gas $\gamma = (d\ lnP/d\ ln\rho)_{ad} = C_P/C_V = (\ell+2)/\ell$ (ℓ is the number of degrees of freedom of a particle) and the magnitude of the cooling represented by a parameter γ^* satisfying $1 \leq \gamma^* \leq \gamma$ (for $\gamma^* = 1$, the cooling goes to infinity and $\alpha \to 2/(2+3\gamma)$ and for $\gamma^* = \gamma$ there is no cooling and $\alpha = 2/5$). The evolution of the ionizing BW is resumed in Figure 1. In the early stage (shell on the left), the expansion velocity is high, the Mach number M is large and ionization effects are small. In the intermediate stage (shell in the middle), the Mach number gets closer to the critical Mach number M_{crit} where ionization effects are strong (see the definition (27) later in II C) and the ionization cooling at the shock front compresses the matter to form a thin and dense shell. Finally, the Mach number is low at late stages (shell in the right). Thus, the ionization effects can be neglected again and the compression of the shell decreases.

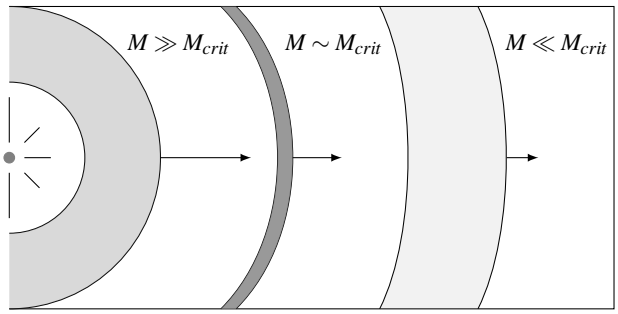

FIG. 1. Sketch of the BW expansion. Three different stages of the shell are represented from left to right. When the Mach number M gets closer to the critical Mach number (see the definition (27) in II C), the ionization cooling is strong and forms a thin and dense shell (shell in the middle).

This paper is organized as follows. In section II, we derive the modified Rankine-Hugoniot relations including ionization

processes and we solve these relations coupled to the Saha equation providing the degree of ionization for a steady ionizing shock wave. We derive the ratios for the thermodynamic and hydrodynamic quantities at the shock front and emphasis is given to the value of the density contrast C in terms of the shock Mach number M. In addition, a critical value of the Mach number, M_{crit} is evidenced. In section III, the model is simplified and the ionization effects are taken into account using an effective adiabatic index only. It is seen that for laser energies from 10 J to 1 kJ, ionization can lead to the formation of a thin and dense shell with a high value of C. In section IV, the dynamics of the BW is studied. Referring to a model developed by Sedov [6] and Barenblatt [32], we derive the value of the expansion rate α driven by ionization and the whole downstream flow (velocity, density and pressure profiles) within the BW is calculated. Our conclusions follow in Section V and special comments about the stability of the ionizing shells and the role of the magnetic field are raised.

II. THE IONIZING SHOCK JUMP EQUATIONS

A. Ionization model for hydrogen gas

First of all, we give the characteristics of the gas in which the BW propagates due to the explosion. In what follows, we will consider a standard laboratory initial condition with a neutral gas of atomic hydrogen where mass density is $\rho_1 = 10^{-3}\,\mathrm{kg/m^3}$ (the corresponding particle density is $n_1 \approx 6\times10^{17}\,\mathrm{cm^{-3}}$) and temperature is $T_1 = 300\,\mathrm{K}$. These values are representative of typical experimental conditions[16,17,20,21]. Now that the initial medium is defined we suppose the propagation of a locally plane stationary shock in it using a hydrodynamical description. In the following, we consider the gas as ideal. When the shock wave is strong enough, the hot postshock medium can be ionized. Although the gas is found in the form of H_2 in the laboratory, for the sake of clarity and simplicity, we will not discuss the dissociation of molecules because it occurs at lower temperatures than ionization and can be neglected at first approximation during the lifetime of the BW. Actually, we will see later (see (27) in Section II C) that the shock velocity at which the ionization effects are important is only proportional to the ionization energy of hydrogen (independently of the initial density and temperature of the gas). We would find in the same way that this is also true during the dissociation of the molecule. Thus, dissociation effects are strong for lower shock velocities independently of the initial state of the gas as the dissociation energy is about three times smaller than the ionization one. We will also suppose that the gas is at local thermodynamic equilibrium (LTE)[33,34], and, therefore, the populations for each species are determined by collisions and they obey a Boltzmann distribution. The same assumption is used by Robinson and Pasley [30] in their numerical study. From the equation of Saha, the populations of atoms, H, protons, H^+, and electrons, e, in the postshock medium satisfy[33],

$$\frac{n_e n_{H^+}}{n_H} = \frac{(2\pi m_e kT)^{3/2}}{{h_P}^3}\exp\left(-\frac{E_{ion}}{kT}\right) \tag{1}$$

where n_e, n_{H^+} and n_H are respectively the numerical densities of electrons, protons ($n_e = n_{H^+}$) and hydrogen atoms, m_e is the mass of the electron, h_P the Planck constant, k is the Boltzmann constant, T is the temperature and E_{ion} is the ionization energy of hydrogen, namely $E_{ion} = 13.6\,\mathrm{eV}$, for numerical application. When the shock propagates into the gas, the shocked medium is partially or totally ionized for a strong enough shock wave. A part of the energy transmitted by the shock will be used to ionize the gas instead of heating it. Moreover, the equation of state for an ideal gas gives the relation $P \propto \rho T$ where P is the pressure and ρ is the mass density. Therefore, the temperature drop will be compensated by an increase in density in order to keep an almost uniform pressure. This compression can be applied to the BW where we expect the shell to be dense and thin due to ionization effects.

B. The generalized jump equations

In contrast to a situation with no ionization, the determination of the physical quantities (mass density, pressure, velocity, temperature, electron density ...) in an ionizing postshock gas is not a trivial matter. Indeed, for a material undergoing no ionization, the modeling is quite simple because the pressure, density, temperature, and velocity in the downstream flow just behind the shock front can be derived from the so-called three Rankine–Hugoniot equations[33] once the equation of state (EoS) is specified. These three equations account for the mass, momentum, and energy conservation and in a frame attached to the shock front they read (the subscripts "1" and "2" stand respectively for the non-shocked (upstream flow) and for the shocked gas (downstream flow)),

$$\rho_2 u_2 = \rho_1 u_1 \tag{2}$$

$$\rho_2 u_2^2 + P_2 = \rho_1 u_1^2 + P_1 \tag{3}$$

$$h_2 + \frac{1}{2}u_2^2 = h_1 + \frac{1}{2}u_1^2 \tag{4}$$

where ρ, u, P and h represent respectively the mass density, the velocity, the pressure and the enthalpy per unit mass in the flow. The EoS provides a relation between ρ, P and the internal energy per unit mass, ε, which is always connected to h through the equation,

$$h = \varepsilon + \frac{P}{\rho}. \tag{5}$$

As a result, for simple EoS and especially for an ideal gas, ρ_2, P_2, T_2 and u_2 can be written analytically in terms of the upstream flow quantities ρ_1, P_1, T_1 and $u_1 = -D$ where D corresponds to the shock front velocity.

For a gas experiencing ionization, Eqs. (2)–(4) actually still holds, however, the resolution is no longer analytical because one faces two additional difficulties. On the one hand, the Rankine–Hugoniot and the Saha equations should be solved numerically at the same time in order to get values of n_e, n_{H^+} and n_H in the shocked material consistent with its temperature, and, on the other hand, ε should contain a term (and so is the same for h in Eq. (5)) that accounts, first for the amount of energy used to ionize the post-shock gas and which depends upon n_e and, second, for the thermal energy of the free electrons. With the above assumption of an ideal gas, the EoS writes,

$$P_i = \frac{\rho_i k T_i}{m_i}, \;\; i = 1,2 \tag{6}$$

where m_i is the average mass per particle. In the ambient gas, we have $m_1 = m_p$ where m_p is the mass of the proton, while in the downstream flow, m_2 is given by,

$$m_2 = \frac{m_p + f_2 m_e}{1+f_2} \approx \frac{m_p}{1+f_2} \tag{7}$$

where m_e has been neglected with respect to m_p and where the ionization fraction f_2 is defined as:

$$f_2 = \frac{n_e}{n_H + n_{H^+}} = \frac{n_{H^+}}{n_H + n_{H^+}}. \tag{8}$$

In this equation, the particle densities n_e, n_{H^+} and n_H are calculated in the shocked material "2" and the ionization fraction satisfies $0 \leq f_2 \leq 1$ (for $f_2 = 0$, no ionization occurs and for $f_2 = 1$ the plasma is fully ionized). Moreover, since the gas is composed of atoms, electrons and protons, with only three degrees of freedom for each of them (mono-atomic gas), we get,

$$\varepsilon_1 = \frac{3P_1}{2\rho_1}. \tag{9}$$

and Eq. (5) gives,

$$h_1 = \frac{5P_1}{2\rho_1}. \tag{10}$$

However, in the downstream flow, the ionization energy should be included in the internal energy, *i.e.*,

$$\varepsilon_2 = \frac{3P_2}{2\rho_2} + \varepsilon_{ion} \tag{11}$$

leading to:

$$h_2 = \frac{5P_2}{2\rho_2} + \varepsilon_{ion} \tag{12}$$

where the requested amount of energy, ε_{ion}, to ionize a unit mass of gas behind the shock front writes,

$$\varepsilon_{ion} = \frac{f_2 E_{ion}}{m_p}. \tag{13}$$

Finally, the dependence of f_2 upon ρ_2 and T_2 can be derived from the Saha equation (Eq. (1)). Using (7) and (8) and the standard equality $\rho_2 = (n_H + n_{H^+} + n_e)m_2$, one obtains the relation,

$$\frac{{f_2}^2}{1-f_2} = \frac{m_p}{\rho_2} \frac{(2\pi m_e k T_2)^{3/2}}{{h_P}^3} \exp\left(-\frac{E_{ion}}{kT_2}\right). \tag{14}$$

Together with (14), Eqs. (2), (3) and (4) provide four equations for the four quantities u_2, ρ_2, T_2 (the elimination of P_2 can be made by using the EoS (6)) and f_2 that depend upon ρ_1, T_1 and the shock front velocity D. The major difficulty arising in the above-mentioned four equations comes from the self-consistent, implicit character of the solution. For instance, f_2 is a function of T_2 from (14) (it depends also on ρ_2) but, on the other hand, the determination of T_2 from the energy equation (4) depends upon f_2 through the energy ε_{ion} in h_2. In our approach, we are going to simplify as much as possible the derivation of the solution and we are going to reduce the system of four equations to a single equation governing the temperature T_2 just behind the shock. This equation comes out from (14) provided both the ionization fraction f_2 and the mass density ρ_2 are expressed in terms of T_2. This procedure is explained in Appendix A. Once T_2 is obtained in terms of ρ_1, T_1 and D, the derivation of f_2, ρ_2 (and P_2), and u_2 is straightforward (see after). For the sake of clarity, let us remind the dimensionless quantities (A1) defined in Appendix A,

$$\eta_2 = \frac{\rho_1}{\rho_2}, \qquad \theta_2 = \frac{T_2}{T_1}, \qquad M = \frac{D}{c_1}, \tag{15}$$

where M is the Mach number and c_1 is the sound speed. From their definitions, M, θ_2 and η_2 satisfy the inequalities $M \geq 1$, $\theta_2 \geq 1$ but $\eta_2 \leq 1$, and a strong shock wave obeys the condition $M \gg 1$. From Appendix A, we can eliminate f_2 between the equations (A4) and (A5) and we are left with a second-degree equation, the solution of which provides the expression of η_2 in terms of θ_2,

$$\begin{aligned} &\eta_2 \equiv F_1(\theta_2) = \\ &\frac{1}{20M^2(a_{ion}+2\theta_2)} \left\{ (3+5M^2)(2a_{ion}+5\theta_2) - \sqrt{G} \right\}, \end{aligned} \tag{16}$$

where the dimensionless ionization energy a_{ion} is given by (A6) and where G writes

$$\begin{aligned} G &= 15(15M^4 - 2(16a_{ion}+15)M^2 + 15)\theta_2^2 \\ &+ 60a_{ion}(5M^4 - 4a_{ion}M^2 + 3)\theta_2 \\ &+ 4a_{ion}^2(5M^2+3)^2. \end{aligned} \tag{17}$$

The solution goes to $\eta_2 = 1/4$ for $M \to +\infty$. This is consistent with the compression ratio of an adiabatic strong shock in an ideal mono-atomic gas. Indeed the effect of ionization is negligible in this asymptotic case (this will be discussed later

with the results). In order to get f_2 as a function of θ_2, we use (16) into (A7) and get,

$$f_2 \equiv F_2(\theta_2) = \frac{1}{120M^2(a_{ion}+2\theta_2)^2}\Big\{-480M^2\theta_2^2 + 15(5M^4+2(15-8a_{ion})M^2-3)\theta_2 + 2a_{ion}(25M^4+120M^2-9)+(5M^2+3)\sqrt{G}\Big\}. \quad (18)$$

In the last step of the calculation, we use Saha equation (14) the solution of which is (the solution with a minus sign in front of the square root is unphysical),

$$f_2 = \frac{A(\theta_2,\eta_2)}{2}[-1+\sqrt{1+4/A(\theta_2,\eta_2)}], \quad (19)$$

where $A(\theta_2,\eta_2)$ is given by the expression (we have used definitions (15)),

$$A(\theta_2,\eta_2) = \kappa\eta_2{\theta_2}^{3/2}\exp(-a_{ion}/\theta_2), \quad (20)$$

with

$$\kappa = (m_p/\rho_1)(2\pi m_e kT_1)^{3/2}/{h_P}^3. \quad (21)$$

In equation (20), the constants κ and a_{ion} depend only on the physical characteristics of the upstream gas. Finally, the equation governing the dimensionless temperature θ_2 is obtained from (19) by replacing η_2 and f_2 by their expressions $F_1(\theta_2)$ (see Eq. (16)) and $F_2(\theta_2)$ (see Eq. (18)), respectively. This non-linear equation for θ_2 which reads,

$$F_2(\theta_2)+\frac{A[\theta_2,F_1(\theta_2)]}{2}\{1-\sqrt{1+4/A[\theta_2,F_1(\theta_2)]}\}=0, \quad (22)$$

is solved numerically and the solution provides the downstream temperature θ_2 in terms of the Mach number M.

C. The results for the postshock medium

The results for the postshock medium "2" are presented in figures 2 - 5. Figure 2 shows the temperature ratio θ_2 as a function of the Mach number M. The dashed curve corresponds to the solution of the classical Rankine – Hugoniot equations, *i.e.* adiabatic shock where ionization is dropped ($E_{ion}=0$). Setting $f_2=0$ in Eqs. (A4) and (A5), and eliminating η_2 between the two equations, one obtains,

$$\theta_2 = \frac{(5M^2-1)(M^2+3)}{16M^2} \quad (23)$$

and asymptotically ($M\to+\infty$), θ_2 behaves like,

$$\theta_2 \approx \frac{5}{16}M^2. \quad (24)$$

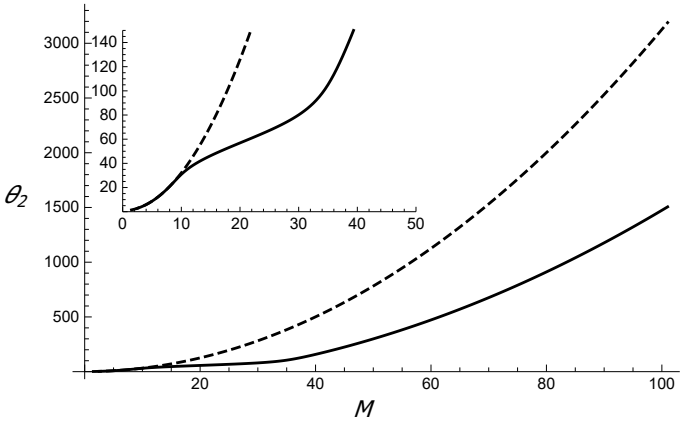

FIG. 2. Temperature ratio θ_2 with ionization ($E_{ion}=13.6\,$eV, solid line) and without ionization ($E_{ion}=0$, dashed line) versus Mach number M for standard experiment conditions ($T_1=300\,$K and $\rho_1=10^{-3}\,$kg/m^3).

This formula gives $\theta_2=3125$ for $M=100$ in agreement with the dashed curve. The solid line gives the solution of the Rankine – Hugoniot equations when ionization is included ($E_{ion}=13.6$ eV). For $M<10$, the two curves superimpose (see the inset) implying that the fraction of ionized atoms is negligible, $f_2\simeq 0$ (see Fig. 3 just after). For increasing M ($M\geq 10$), the temperature increases much less than for a shock without ionizing effects. This result is interpreted physically by the fact that ionization consumes a part of the energy delivered by the shock wave which should normally be used to heat the gas. Finally, for $M\to+\infty$, we have again $\theta_2\propto M^2$ like in an adiabatic shock because the energy requested to ionize the atoms becomes negligible compared to the thermal energy in the medium "2". Nevertheless, in comparison to Eq. (24) the proportionality coefficient is twice smaller because when the gas is totally ionized, there are twice more particles to heat (the coefficient $5/32$ instead of $5/16$ is easily recovered from Eqs. (A4) and (A5) where we set $f_2=1$ and where we neglect the term $2f_2\,a_{ion}/5$). Indeed, for $M=100$, we get $\theta_2\sim 1500$. Figure 3 exhibits the ionization fraction f_2 as a function of M for various values of the density ρ_1 and the ionization energy E_{ion}. On the one hand, it is clear that the denser the gas is, the smaller the ionization fraction is. This property comes out from Eq. (21) where we see that for increasing values of ρ_1, κ decreases and so does f_2. For $\rho_1=10^{-3}\,$kg/m^3 (solid line), the gas is fully ionized for $M\approx 35$ while for $\rho_1=0.1\,$kg/m^3 (dotted line) complete ionization occurs for $M\approx 55$. On the other hand, if the ionization energy is decreased ($E_{ion}=9\,$eV, dashed line), full ionization happens for a smaller M because less energy is needed to ionize medium "2".

The compression ratio C_2 is defined as $C_2=1/\eta_2=\rho_2/\rho_1$ and it is exhibited in Fig.4 for three values of the ionization energy plus a curve for the case without ionization which is given by,

$$C_2 = \frac{4M^2}{3+M^2}. \quad (25)$$

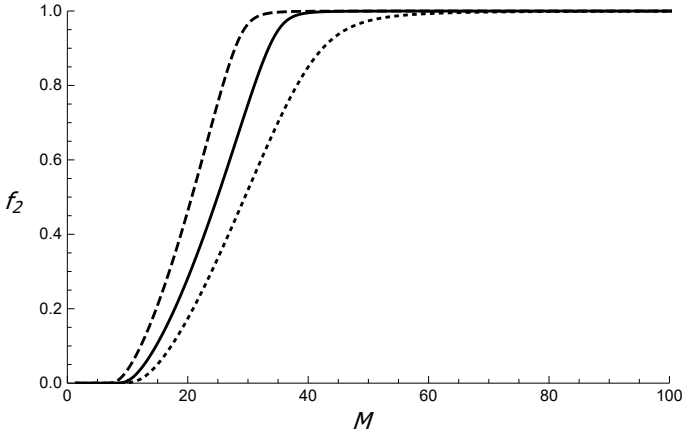

FIG. 3. Ionization fraction f_2 versus Mach number M for different value of ionization energy and initial density: $E_{ion} = 13.6\,\mathrm{eV}$ and $\rho_1 = 10^{-3}\,\mathrm{kg/m^3}$ (solid line), $E_{ion} = 13.6\,\mathrm{eV}$ and $\rho_1 = 0.1\,\mathrm{kg/m^3}$ (dotted line) and $E_{ion} = 9\,\mathrm{eV}$ and $\rho_1 = 10^{-3}\,\mathrm{kg/m^3}$ (dashed line). For the three cases the upstream temperature is $T_1 = 300\,\mathrm{K}$.

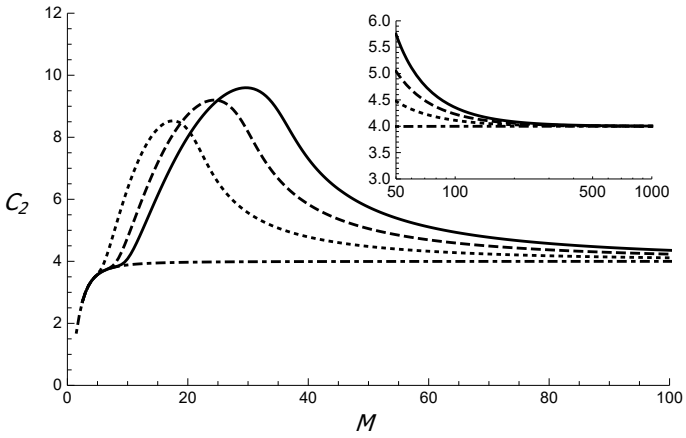

FIG. 4. Compression ratio C_2 versus Mach number M for different value of ionization energy: $E_{ion} = 13.6\,\mathrm{eV}$ (solid line), $E_{ion} = 9\,\mathrm{eV}$ (dashed line), $E_{ion} = 4.5\,\mathrm{eV}$ (dotted line) and $E_{ion} = 0$ (dotted-dashed line) with standard initial experiment conditions ($T_1 = 300\,\mathrm{K}$ and $\rho_1 = 10^{-3}\,\mathrm{kg/m^3}$).

This expression comes directly from the classical Rankine-Hugoniot equations ($f_2 = 0$). For $M \gg 1$, we recover $C_2 = 4$ which corresponds to the value for an adiabatic shock into a mono-atomic gas as mentioned earlier. The three other curves show a high peak from 8.5 to 9.5 for a Mach number in the range $17 \leq M \leq 30$. This behavior is directly due to ionization and the physical interpretation is similar to the one we have explained for the temperature in Fig. 2. Indeed, since a non-negligible fraction of the energy released by the shock wave is used to remove electrons from the atoms, the downstream flow is not heated as it should be with no ionization and, consequently, the compressibility becomes very large. From Fig.4, it turns out that the peak value is slightly sensitive to the ionization energy E_{ion} where the compression increases with increasing values of E_{ion}. Also, it is evidenced that the value of the Mach number for which C_2

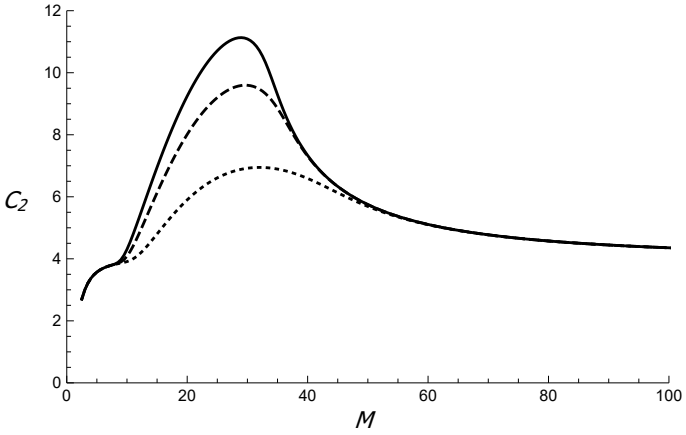

FIG. 5. Compression ratio C_2 versus Mach number M for different value of the initial density: $\rho_1 = 10^{-4}\,\mathrm{kg/m^3}$ (solid line), $\rho_1 = 10^{-3}\,\mathrm{kg/m^3}$ (dashed line) and $\rho_1 = 0.1\,\mathrm{kg/m^3}$ (dotted line) for $T_1 = 300\,\mathrm{K}$ and ionization energy $E_{ion} = 13.6\,\mathrm{eV}$.

has its peak increases with E_{ion}. For $E_{ion} = 13.6\,\mathrm{eV}$, $C_2 \approx 9.5$ at $M \approx 30$ and for such a value of the Mach number, full ionization is achieved (see Fig. 3). For $E_{ion} = 4.5\,\mathrm{eV}$ (resp. $E_{ion} = 9\,\mathrm{eV}$) the peak occurs at $M \approx 17$ (resp. $M \approx 25$). For actual ionization of hydrogen ($E_{ion} = 13.6\,\mathrm{eV}$), the peak arises for a shock front velocity $D \approx 60\,\mathrm{km/s}$ (we have used the sound velocity $c_1 \approx 2030\,\mathrm{m/s}$ from Eq. (A2)). Finally, when the Mach number becomes very large ($M \simeq 100$), the energy used to ionize the atoms becomes small compared to the thermal energy and C_2 tends to 4 (see above). Although f_2 does not satisfy anymore $f_2 = 0$ like for an adiabatic shock, this result is again immediately derived from (A4) and (A5) where the product $(1 + f_2)\,\theta_2$ is eliminated between the two equations and where $2 f_2\, a_{ion}/5$ is neglected with respect to the term proportional to M^2. Besides, the effect of the initial mass density of the gas is studied in Fig. 5. It is seen that the magnitude of the peak increases for decreasing mass density and C_2 reaches a value of 11 (resp. 7) for $\rho_1 = 10^{-4}\,\mathrm{kg/m^3}$ (resp. $\rho_1 = 0.1\,\mathrm{kg/m^3}$). In a similar way to what happens in figure 3, when ρ_1 increases, f_2 decreases. As a consequence, the amount of energy used to ionize the material remains small compared to the thermal energy and the compression is low. The high value $C_2 \approx 11$ shown in Fig. 4 is therefore due to the low density of the gas. However one has to be careful that there is a lower limit of initial density below which the validity of the LTE would fall in the shocked medium. This lower threshold is rather complicated to find and also depends on the plasma temperature. Although its determination goes beyond the scope of this article, below $\rho_1 \sim 10^{-5}\,\mathrm{kg/m^3}$, the LTE assumption would probably be already incorrect behind the shock[35].

Let us come back to the value of M (this value is called M_{crit} hereafter) for which C_2 shows a peak. We give a rough estimation of M_{crit} from elementary theoretical considerations. We introduce the ratio δ between the ionization energy E_{ion} and the kinetic energy of an atom that is roughly given by $m_p D^2/2$.

Using the equalities $D = Mc_1$ and $c_1 \approx (kT_1/m_p)^{1/2}$ (see Eq. (A2)), one gets,

$$\delta \approx \frac{2E_{ion}}{M^2 kT_1} \tag{26}$$

Clearly, full ionization occurs for $\delta \approx 1$ and, therefore, M_{crit} satisfies,

$$M_{crit} = \sqrt{\frac{2E_{ion}}{kT_1}}. \tag{27}$$

For the standard conditions of the gas we have taken in this paper ($T_1 = 300\,\mathrm{K}$ and $\rho_1 = 10^{-3}\,\mathrm{kg/m^3}$) with $E_{ion} = 13.6\,\mathrm{eV}$, Eq. (27) gives

$$M_{crit} \approx 32. \tag{28}$$

This value is actually close to the value derived from the solid curve in Fig. 4.

III. SIMPLIFIED ANALYSIS OF IONIZING SHOCKS AND APPLICATION TO BW IN LABORATORY

A. The evolution of the BW in laboratory

From section II, it turns out that a key value of the Mach number is $M_{max} \approx 30$ (this value is close to the value M_{crit}) since it achieves the maximum compression ratio ($C \approx 9.5$ in Fig. 5) and, therefore it can potentially alter the evolution of the BW. As shown earlier, the calculation of this value is however not trivial because the procedure should take into account the temperature and the ionization fraction in the postshock material in a self-consistent way. The purpose of this section is twofold. First, we examine how much such a value of M is relevant for experimental conditions of a laser-induced BW. Second, an alternative approach to the procedure developed in Section II is presented. This second approach is first fully analytic and second, although it is somewhat less accurate than the first one, especially regarding the value of the postshock temperature, a rather exact value of the compression ratio at the shock front can be obtained once the ratio of the specific heats (at constant pressure and at constant volume) of the partially (or fully) ionized material has been calculated. Finally, this derivation is going to be used in the next section (Section IV) in order to implement a model developed by Barenblatt and Sivashinskii [36] several years ago. In the experiments by Grun *et al.* [16], Edens *et al.* [18], Riley *et al.* [20], Edens *et al.* [21], the propagation of a laser-induced BW is observed for a typical duration of a few nano-seconds using energy laser from 10 J to 1 kJ. In all those papers, the authors demonstrate the strong effects of radiative cooling on the evolution, internal structure and stability of the BW. This scenario has been studied first in the context of SNR radiative stage[37–39]. The major effects of cooling are, first, an expansion of the SNR that is more decelerated than in the adiabatic Sedov-Taylor regime[12,38,40] and, second, the presence of internal shocks inside the SNR[38,41,42] and the formation of a dense shell at its outer border[38,43,44]. In what follows, we will only consider the case of a non-radiative BW. Under this assumption, the time variation of the BW radius is given by the Sedov-Taylor law :

$$R_{ST} = \xi_0 (\frac{E_0}{\rho_1})^{1/5} t^{2/5} \tag{29}$$

where $\xi_0 \approx 1.15$ is a dimensionless number[45] and $E_0 \approx 1\,\mathrm{kJ}$ is the laser energy release. For the conditions of the standard ambient gas that we consider ($T_1 = 300\,\mathrm{K}$ and $\rho_1 = 10^{-3}\,\mathrm{kg/m^{-3}}$, see section II), we find that the Mach number evolves as

$$M(t) \approx 3.5 \times 10^{-5} t^{-3/5} \tag{30}$$

where t should be expressed in second. Therefore, when $M = M_{crit} \approx 30$ (strongest ionization effects), the age of the BW is around $t_{crit} \approx 300\,\mathrm{ns}$ and the radius is around 40 mm. This result is close to the experiment in nitrogen by Edens *et al.* [21] where the radius is 30 mm at 300 ns for similar conditions of the initial gas state and laser energy. Notice that the similarity property of (29) implies that the same BW configuration (duration, size, velocity and Mach number) can be achieved for the same initial ratio E_0/ρ_1. As the decrease in the initial density is limited to order of magnitude $\rho_1 \sim 10^{-5}\,\mathrm{kg/m^{-3}}$ to stay in the LTE regime (see in section II C), the minimum laser energy can decrease to about 10 J.

B. Simplified ionizations jump condition for the BW

The purpose of this paragraph is to propose a simplified analytical approach to reduce the complexity of the model. As we suppose that the gas is composed of hydrogen atoms, the partially ionized shocked medium is then composed of hydrogen atoms, protons, and electrons, and the adiabatic index of medium "1" and "2" equals $5/3$ which is the value for a mono-atomic gas. Indeed, the adiabatic index is related to the number of degrees of freedom ℓ of the gas particles. In the present case, $\ell = 3$ so $\gamma = (\ell+2)/\ell = 5/3$. However, due to ionization, deviations to the mono-atomic ideal gas arise in the energy balance (see for instance Eq. (11)). As a consequence, we define a new effective adiabatic index γ^*[33,46] which takes into account the ionization effects in medium "2" through the equation,

$$\varepsilon_2 = \frac{1}{\gamma^* - 1}\frac{p_2}{\rho_2} = \frac{3}{2}\frac{p_2}{\rho_2} + \varepsilon_{ion} \tag{31}$$

where the adiabatic index $\gamma^* \neq 5/3$. In general, the function $\gamma^*(T_2, \rho_2)$ depends on the temperature and the density of the shocked medium. Nevertheless, instead of T_2 and ρ_2, it can be shown that γ^* can be expressed actually in terms of the temperature ratio θ_2 and the ionization fraction f_2 only. Indeed, using the ionization energy definition (13) and (31), we finally obtain the analytical formula,

$$\gamma^* = \frac{5(1+f_2)\theta_2 + 2a_{ion}f_2}{3(1+f_2)\theta_2 + 2a_{ion}f_2}\,. \tag{32}$$

One can notice that when we suppress ionization (either $f_2 = 0$ or $a_{ion} = 0$), we recover the value $\gamma^* = 5/3$ for a mono-atomic gas. Similarly, when the thermal energy of the shocked medium is high compared to the ionization energy $\theta_2 >> a_{ion}$ we also find $\gamma^* \simeq 5/3$. We are going to make an additional assumption noticing that for a given temperature, the ionization fraction varies slowly with the density in the range $\rho_1 < \rho < \rho_2$. Indeed, the density ρ_2 is bounded by the upper value $\rho_2 = \rho_1 M^2$ which corresponds to $\gamma^* = 1$ and the variations of f_2 when ρ varies from ρ_1 to ρ_2 can be neglected in first approximation (see the variations of f_2 in figure 3 where ρ_1 is changed). Thus, we can write $f_2(\theta_2, \eta_2) \simeq f_2(\theta_2, 1)$ (see Eq.(19)) and as a consequence the quantity γ^* only depends on the dimensionless temperature θ_2. The effective adiabatic index is plotted for the standard experiment conditions in figure 6 where as expected we recover the value $5/3$ for $\theta_2 \to 1$ and $\theta_2 \to +\infty$. Notice that γ^* reaches the minimal value 1.2, which gets closer to the limit $\gamma = 1$ where all the shock energy is used to ionize the gas instead of heating it ($\theta_2 << a_{ion}$). This limit corresponds to the so-called isothermal shock for which $T_2 \simeq T_1$ ($\theta_2 \simeq 1$). The variation of γ^* is very sharp for $30 < \theta_2 < 40$ but the index increases rather slowly in the range $50 < \theta_2 < 200$. As it can be deduced from Fig. 2, this range is achieved for a Mach number about $M \simeq 20 - 50$ which is relevant to a laser-induced BW in the laboratory as explained from Eq. (30). Consequently, we can consider in the first approximation that γ^* is almost constant during the evolution of the ionizing BW. This assumption will be discussed in the next section. Now that we have defined a new effective adiabatic index γ^* for medium "2" different from the adiabatic index (denoted $\gamma_1 = 5/3$) for medium "1", we will determine again the state of the shocked medium using the classical Rankine-Hugoniot equations with different adiabatic indices for medium "1" and "2". In the present case, the ionization energy is still taken into account in the energy equation (4) (in the enthalpy h_2) but it contributes implicitly through the value of γ^*. Then, combining (31) and (5), the downstream enthalpy writes,

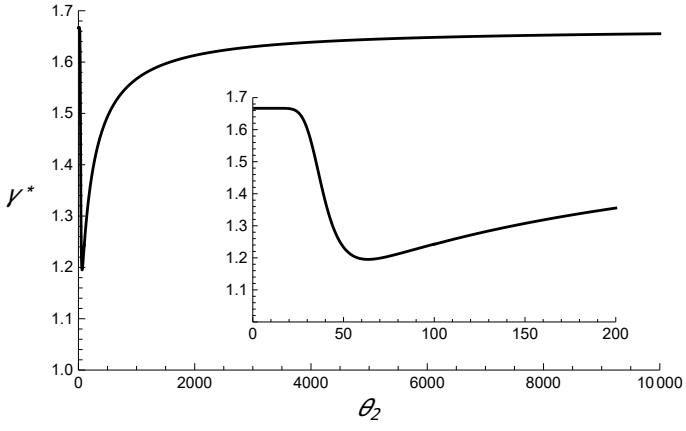

FIG. 6. Effective adiabatic index γ^* versus the dimensionless temperature θ_2 for the experiment conditions ($T_1 = 300\,\mathrm{K}$ and $\rho_1 = 10^{-3}\,\mathrm{kg/m^{-3}}$).

$$h_2 = \frac{\gamma^*}{\gamma^* - 1}\frac{P_2}{\rho_2}\,. \tag{33}$$

Finally, the state of medium "2" can be determined from the Rankine-Hugoniot equations following the calculations by Sedov[6] or by Drake[46] and, especially, the compression ratio reads,

$$C_2 = \frac{\gamma^*(\gamma_1 - 1)(1 + \gamma_1 M^2) + \sqrt{J}}{\gamma_1(\gamma^* - 1)[2 + (\gamma_1 - 1)M^2]} \tag{34}$$

where

$$J = (\gamma_1 - 1)[(\gamma_1 - 1)(\gamma^{*2} + \gamma_1^2 M^4) + 2\gamma_1(\gamma_1 - \gamma^{*2})M^2]\,. \tag{35}$$

At this stage, we should specify that the state of the shocked medium is not completely determined. Indeed, the function $\gamma^*(\theta_2)$ still depends on the temperature of the medium "2". Thus, similarly to the previous section, the algebraic system is non-linear and needs to be solved numerically. However, it is important to notice two points. First, if the shock is strong enough ($M \gg 1$), which is the case for a BW considered here, equation (34) reduces to the asymptotic expression $C_2 = (\gamma^* + 1)/(\gamma^* - 1)$ irrespectively of the value of γ_1. This expression is the same as the one derived for an adiabatic strong shock except that $\gamma^* \neq \gamma_1$. We can deduce that for a strong shock, the compression ratio only depends on the adiabatic index of the shocked medium. If this index drops to a value close to 1, the compression ratio will become very large. Moreover, we know the analytical expression for γ^* in terms of temperature ratio θ_2. Inserting (32) in the above asymptotic expression of C_2, one gets,

$$C_2(\theta_2) \simeq \frac{\gamma^*(\theta_2) + 1}{\gamma^*(\theta_2) - 1} = 4 + \frac{2a_{ion} f_2(\theta_2)}{[1 + f_2(\theta_2)]\theta_2}, \tag{36}$$

for $M >> 1$ and $\gamma_1 = 5/3$. In this analytical formula, the second term on the right-hand side highlights the properties that need to be satisfied in the initial medium "1" to increase the compression ratio at the shock front. A similar formula is also found in the book by Zel'Dovich and Raizer[33]. First, for a given dimensionless ionization energy a_{ion}, the dimensionless temperature θ_2 needs to be low enough to verify the condition $a_{ion}/\theta_2 \gg 1$ (ionization energy greater than thermal energy). The ionization also needs to operate at this low temperature to verify the second condition $f_2(\theta_2) \sim 1$. Thus, having both the combination of high ionization energies and ionization processes occurring at low temperatures, the term $2a_{ion} f_2/[(1 + f_2)\theta_2]$ will be large and the compression ratio will be large as well. These conditions can be fulfilled for rarefied gas. In figure 7, we compare the compression ratio computed numerically from section 2 and the analytical formula (36) (assuming a high Mach number) using the same initial conditions for the ambient gas. Notice the good agreement between the two curves when the Mach number becomes

high ($M > 50$), *i.e.* for large values of θ_2. The difference in the two curves at the maximum of compression is due to the assumption $f_2(\theta_2,\eta_2) \simeq f_2(\theta_2,1)$. By not taking into account the compression in the shocked medium ($\eta_2 = 1$), we slightly overestimate the degree of ionization in this medium and from (36) this implies a greater compression. If we use the minimum value of $\gamma^* \simeq 1.2$ (see figure 6) in the standard experiment conditions, we find the maximum compression ratio $C_2 = 11$. Finally, one could go further in the simplification of the model and consider that γ^* is constant in a given range of θ_2 (here between 40 and 200)[33]. We recognize that this approximation of the shocked medium for a Mach number close to M_{crit} is rather drastic, however, we will see in the next section this is the price to pay for applying the model by Barenblatt [32] for a self-similar description of the BW including ionization. In a more realistic one-dimensional model taking into account the change of γ^* according to the decrease of the BW Mach number $M(t)$, the numerical solution would move continuously from a self-similar solution to another with a different coefficient γ^*. This is likely to happen because the solution of Barenblatt is stable in the simulations by Andrushchenko, Barenblatt, and Chudov [47]. Thus, the solution will be different from the Sedov-Taylor solution only in the region close to $M = M_{crit}$.

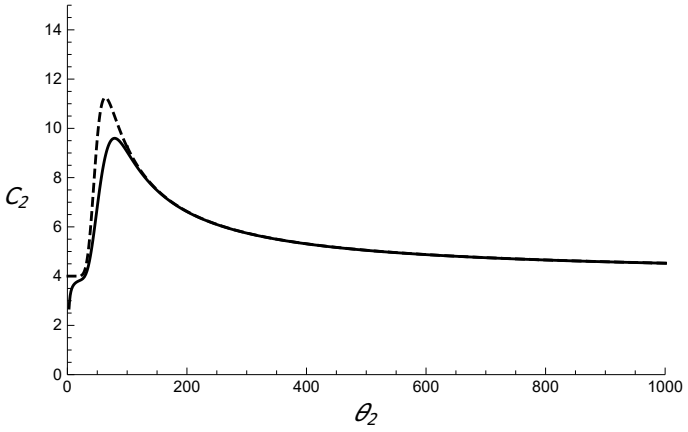

FIG. 7. Comparison between the compression ratio C_2 computed numerically in section II C (solid line) and the formula C_2 (36) (dashed line) versus the dimensionless temperature θ_2.

IV. EVOLUTION AND INTERNAL STRUCTURE OF THE IONIZING BW

In the original model of Barenblatt [32] and an earlier work by Sedov[6], the idea was to describe a blast wave that loses energy by cooling only at the shock front. This is exactly what happens when the shock front of a BW ionizes the ambient gas. To account for this process, the authors introduce an additional constant quantity q in the energy equation according to,

$$\frac{\gamma}{\gamma-1}\frac{p_2}{\rho_2} + \frac{1}{2}u_2^2 - q = \frac{\gamma}{\gamma-1}\frac{p_1}{\rho_1} + \frac{1}{2}u_1^2, \tag{37}$$

where q represents an energy per unit mass. In this section, the pressure will be denoted by p. Notice that in this model, both sides of the front have the same arbitrary adiabatic index gamma. In the present case $q < 0$ as the BW cools at the shock front due to the thermal energy lost to ionize the gas. In order to find self-similar solutions the quantity q should obey the special form[32],

$$q = Q\frac{p_2}{\rho_2}, \tag{38}$$

where Q is a dimensionless negative constant. Plugging this expression in (37), one gets the simplified energy equation,

$$\frac{\gamma^*}{\gamma^*-1}\frac{p_2}{\rho_2} + \frac{1}{2}u_2^2 = \frac{\gamma}{\gamma-1}\frac{p_1}{\rho_1} + \frac{1}{2}u_1^2, \tag{39}$$

with

$$\gamma^* = \frac{(\gamma-1)Q-\gamma}{(\gamma-1)Q-1}. \tag{40}$$

Eq. (39) exhibits two interesting properties. It describes an adiabatic shock wave where the adiabatic index is $\gamma^* \neq \gamma$ in the downstream flow on the one hand, and, on the other hand, it is the same equation as the one derived in the previous section where (33) is inserted in Eq. (4) and where $h_1 = [\gamma/(\gamma-1)]\ p_1/\rho_1$. This result shows that ionization can be described by this model provided the approximation of a constant effective adiabatic index at the shock front of the ionizing BW.

When $Q = 0$, Eq. (40) gives $\gamma^* = \gamma$ and the problem is reduced to the classical strong explosion of Sedov-Taylor where the total energy is conserved during the expansion of the BW. When $Q \to +\infty$, $\gamma^* \to 1$ and corresponds to an infinite cooling at the shock front (we will come back to that point). In this case, the shock is isothermal as described in Sect. III. Finally, as it is done by Barenblatt [32], and as it turns out from the Rankine-Hugoniot equation for a strong shock, the boundary conditions of the BW at the shock front are given by,

$$\rho_2 = \frac{\gamma^*+1}{\gamma^*-1}\rho_1, \quad v_2 = \frac{2}{\gamma^*+1}D, \quad p_2 = \frac{2}{\gamma^*+1}\rho_1 D^2. \tag{41}$$

One can again notice that the state of the shocked medium only depends on the effective adiabatic index which takes into account the effects of ionization in the present situation. It is important to notice that the adiabatic index is $\gamma = 5/3$ inside the BW and is different from γ^* at the shock. Indeed, the temperature in the interior is much higher than the temperature at the shock front. Thus, the index comes back to the adiabatic value of mono-atomic and fully ionized gas (see Figure 6 at

high temperature). The one-dimensional and spherically symmetric hydrodynamic conservation equations of mass, momentum, and energy are,

$$\partial_t \rho + \frac{1}{r^2}\partial_r(r^2\rho v) = 0, \tag{42}$$

$$\partial_t v + v\partial_r v + \frac{1}{\rho}\partial_r p = 0, \tag{43}$$

$$\partial_t(\frac{1}{2}\rho v^2 + \varepsilon) + \frac{1}{r^2}\partial_r[r^2 v(\frac{1}{2}\rho v^2 + \varepsilon + p)] = 0. \tag{44}$$

Following[6,32,48,49], we use the self-similar approach to transform the partial differential equations (42) – (44) in three ordinary differential equations (ODE) – see below. The transformation is

$$\begin{aligned} \rho &= \frac{\gamma^*+1}{\gamma^*-1}\rho_1 R(\xi,\gamma,\gamma^*) \\ v &= \frac{2\alpha}{(\gamma^*+1)}\frac{r}{t}V(\xi,\gamma,\gamma^*) \\ p &= \rho_1\frac{2\alpha^2}{(\gamma^*+1)}\frac{r^2}{t^2}P(\xi,\gamma,\gamma^*) \end{aligned} \tag{45}$$

where R, V, and P are the self-similar density, velocity, and pressure, respectively, and $\xi = r/r_0(t)$ is the self-similar coordinate where $r_0(t)$ is the time-dependent radius of the BW. Following[32], we assume $r_0(t) = At^\alpha$ where A is a constant and where the constant α is called the decelerating parameter. This behavior is similar to the evolution of the Sedov-Taylor blast wave except that $\alpha < 2/5$ when $\gamma^* < \gamma$. Using the transformations (45) in (42)-(44), one gets the three ODE,

$$[\frac{2V-(\gamma^*+1)}{2R}]\frac{dR}{d\ln\xi} + \frac{dV}{d\ln\xi} = -3V \tag{46}$$

$$\begin{aligned} &[\frac{2V-(\gamma^*+1)}{V}]\frac{dV}{d\ln\xi} + \frac{\gamma^*-1}{RV}\frac{dP}{d\ln\xi} \\ &= (\frac{\gamma^*+1}{\alpha} - 2V) - 2\frac{\gamma^*-1}{RV}P \end{aligned} \tag{47}$$

$$\begin{aligned} &[\frac{2V-(\gamma^*+1)}{2P}]\frac{dP}{d\ln\xi} - \gamma[\frac{2V-(\gamma^*+1)}{2R}]\frac{dR}{d\ln\xi} \\ &= (\frac{\gamma^*+1}{\alpha} - 2V) \end{aligned} \tag{48}$$

with the boundary conditions $R(1,\gamma,\gamma^*) = V(1,\gamma,\gamma^*) = P(1,\gamma,\gamma^*) = 1$. The resolution of these ODE is described by Barenblatt[32]. It is shown that for a given value of the effective adiabatic index γ^*, there is a unique solution of the decelerating parameter α where the solution is integrated from the shock front to the center of the BW. This solution with $\alpha = \alpha^*$ is the physically relevant solution obtained from an eigenvalue problem (see below). Indeed, in the simulation by Andrushchenko, Barenblatt, and Chudov[47], the authors demonstrate that a blast wave generated by the release of a huge amount of energy in a small volume using a value of $\gamma^* < \gamma$ at the shock front converges to the special solution $\alpha = \alpha^*$. Close to the center, the asymptotic expansion of the solution reads,

$$\begin{aligned} R &= R_0\xi^s + O(\xi^{2s+2}), \qquad s = \frac{6(1-\alpha^*)}{\alpha^*(2+3\gamma)-2} \\ V &= V_0 + O(\xi^{s+2}), \qquad V_0 = \frac{\gamma^*+1}{2\gamma} + \frac{(2-5\alpha^*)(\gamma^*+1)}{6\alpha^*\gamma} \\ P &= \frac{P_0}{\xi^2} + O(\xi^s), \end{aligned} \tag{49}$$

where R_0 and P_0 are constants which depend on the parameters γ, γ^* and α^*. Thus, the eigenvalue problem can be defined as follows. For a given γ^*, one needs to find the unique solution with the exponent $\alpha = \alpha^*(\gamma^*)$ that goes from the central boundary given by (49) to the boundary at the shock front. We can also see from (49) that the critical expression of the exponent $\alpha^*_{crit} = 2/(2+3\gamma)$ corresponds to the singular limiting case $s \to +\infty$ (Gintrand *et al.*[48]). Actually, Barenblatt[32] shows that α^*_{crit} corresponds to the lower value of $\alpha^*(\gamma^*)$ and it is achieved for $\gamma^* \to 1$. As a consequence, the density R satisfies $R \to 0$ for $\xi \to 0$ and the closer to one γ^* is, the more rarefied the inner part of the BW is: the matter that is swept up by the shock front becomes concentrated in an infinitely thin shell of infinite compression ratio at the front shock. For $\gamma = 5/3$, one gets $\alpha^*_{crit} = 2/7$, *i.e.* $r_0(t) \propto t^{2/7}$, modeling the so-called pressure-driven snowplow (PDS) regime – see the Introduction – which has been extensively studied in the literature since the seventies[7–9] and has been recently recovered analytically for a BW experiencing radiative cooling[48]. Several solutions are plotted in figure 8 for different values of the effective adiabatic index. The lower case $\gamma^* = 1.2 < \gamma = 5/3$ (solid lines) is the minimum value from the previous section. Then the corresponding values of α^* are found through the eigenvalue problem using a trial and error method to converge to the special solution. The compression ratio at the front shock is high with $\rho_2/\rho_1 \approx 11$ and $\rho_2/\rho_1 \approx 6$ for the solid and dashed lines respectively. This is due to the ionization cooling effects and as expected, the shell becomes thinner and denser compared to the Sedov–Taylor case (dotted lines) for which it is reminded that $\rho_2/\rho_1 = (\gamma+1)/(\gamma-1) = 4$. Also, the dimensionless thermal pressure in the hot interior decreases to $p/p_2 = 0.24$ (solid line) and $p/p_2 = 0.27$ (dashed line) at the center compared to the value 0.3 for the Sedov–Taylor solution. In addition, as the total energy of the BW decreases with time, the decelerating parameter $\alpha^* = 0.329$ (solid lines) and $\alpha^* = 0.361$ (dashed lines) are smaller than 2/5. The lowest

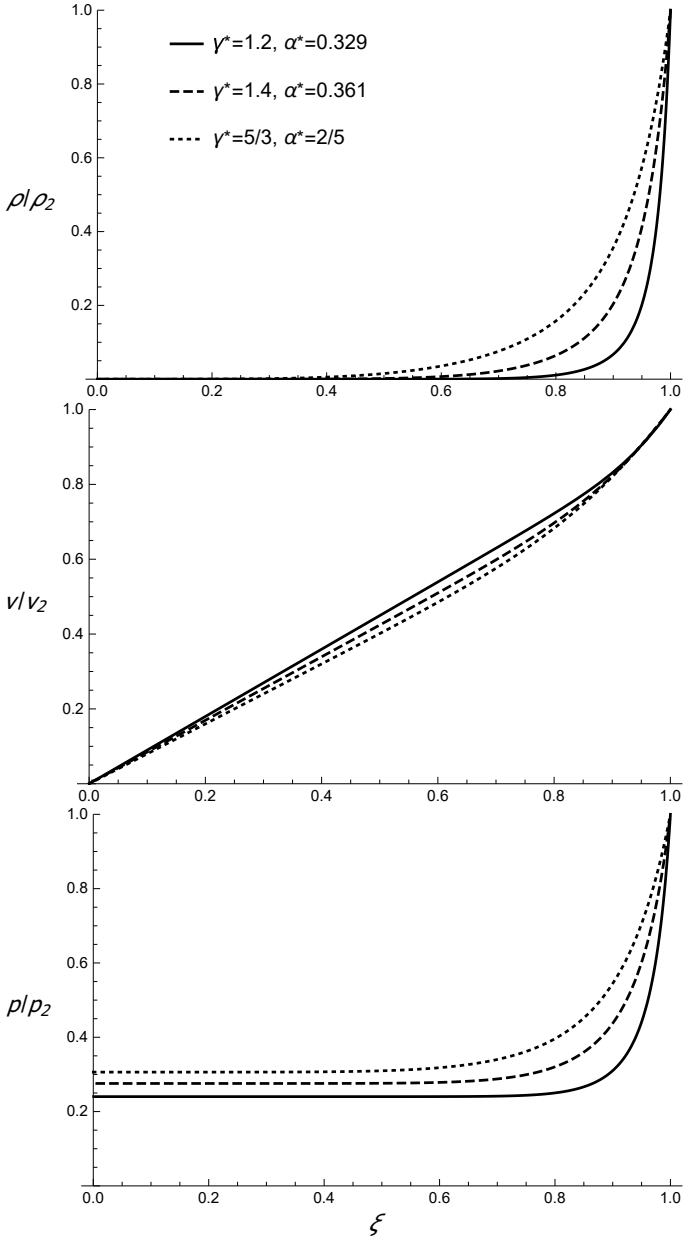

FIG. 8. Normalized profiles of density ρ/ρ_2 (top panel), velocity v/v_2 (middle) and pressure p/p_2 (bottom panel) versus the dimensionless position $\xi = r/r_0$ for different values of the effective coefficient γ^*.

value of α^* is actually similar to the values derived by Blondin *et al.* [38] from the numerical simulations of SNR experiencing energy losses by radiation.

V. CONCLUSION & DISCUSSION

In this article, we have studied the ionization of cold atomic hydrogen by a blast wave (BW). The equations of the analytical model, *i.e.* Rankine–Hugoniot and Saha equations, have been solved in a self-consistent way. In agreement with our expectations raised in the introduction, we have shown that ionization has a significant role in the dynamics and the structure of laboratory BW as the one by Grun *et al.* [16], Edens *et al.* [18,21] and Riley *et al.* [20] using laser energy from 10 J to 1 kJ. We have found that the compression ratio C for an ionizing shock can reach high values (the maximal compression ratio we found is $C \simeq 11$) around a critical Mach number $M_{crit} \simeq 30$ where the gas is almost fully ionized. Indeed, as a fraction of the shock energy is used to ionize the gas instead of heating it, the density needs to increase behind the shock to maintain the value of the pressure in the downstream flow. As a consequence, we might say that ionization is equivalent to some cooling. This ionizing cooling effect gets stronger when the ratio of ionization energy over thermal energy in the shocked region is large during ionization. Thus, for given ionization energy, the ionization needs to be done at low temperatures and this can only be achieved by decreasing the gas density. In the second part, we have introduced an effective adiabatic index γ^* accounting for ionization and we have shown the well-known result that its value drops below 5/3. Actually, formula (32) gives $\gamma^* = 5/3 - 4a_{ion}f_2/\{3[3(1+f_2)\theta_2 + 2a_{ion}f_2]\}$ where index 2 represents the downstream shocked medium. Assuming the strong shock approximation, the compression C is given by $C = (\gamma^*+1)/(\gamma^*-1) > 4$ and it is shown that this expression provides a value close to the one derived from the exact solution of the Rankine–Hugoniot equations including ionization. The minimum value of the effective index is $\gamma^* = 1.2$ and is achieved for $\theta_2 \simeq 60$. Besides, for $M = M_{crit}$ which corresponds to $\theta_2 \simeq 80$ we get $\gamma^* \simeq 1.23$. As a consequence, for $M \simeq M_{crit}$, *i.e.* when ionization dominates the structure and the dynamics of the BW, the variation of γ^* is so little that it can be neglected and we can take a constant value $\gamma^* = 1.2$. Under these circumstances, the structure and the dynamics of the flow inside the whole BW can be described by the self-similar solution derived from the point explosion model of Barenblatt [32] where a uniform pressure but extremely low-density bubble bounded at the shock front by a thin and dense shell are evidenced. The position $r_0(t)$ of the shock front, *i.e.* the radius of the BW, writes $r_0(t) \propto t^{\alpha^*}$ where the value of the deceleration parameter is $\alpha^* = 0.329$. Since it was shown that ionization plays a role equivalent to cooling at the shock front, this value is smaller than $\alpha = 2/5$ corresponding to the Sedov–Taylor BW, as expected. If one can find a configuration of the initial gas state that would increase the post-shock ratio $f_2 E_{ion}/((1+f_2)kT_2)$ (see (36)), the value of the effective index γ^* could decrease even closer to one. The asymptotic regime $\gamma^* = 1$ corresponds to the so-called Pressure-Driven Snowplow (PDS) stage of the BW where the exponent $2/7 \approx 0.286$ is obtained from the theoretical formula $2/(2+3\gamma)$ with $\gamma = 5/3$. Moreover, although $\alpha = 1/4$ (Momentum-Conserving Snowplow (MCS) stage of the BW) comes out when radiative cooling takes place[48], this value does not arise for the case of ionization as there is not any cooling in the BW hot interior but only at the shock front. Also, although the linear stability of this self-similar solution has not been performed yet, it is likely unstable against the so-called Vishniac and Ryu–Vishniac instabilities[40,50–53] which predict unstable evolution for $\gamma < 1.2$. The ionizing

cooling BW may be a better candidate for the study of the Vishniac instability than the radiative cooling as the radiative one may be dominated by thermal and convective instabilities due to the change in the internal structure of the radiative BW[39,48]. In the experiment by Edens *et al.* [18], the 1 kJ laser-induced BW in Nitrogen is simulated using HYADES code with multigroup diffusion for the radiation transport and SESAME tabulated EoS. The results give an effective index $\gamma^* = 1.36$. Even if the ionization cooling of Nitrogen may have played a role in the drop of the effective index, the value of γ^* is still larger than the Vishniac instability threshold ($\gamma = 1.2$) and the perturbed BW seems stable from experimental diagnostics. However, it is important to notice that the stability analysis performed in Ryu and Vishniac [51], Sanz *et al.* [52] is different than the stability of the Barenblatt model discussed in this article where ($\gamma^* < \gamma$). In addition, these ionizing shock waves are liable to the D'yakov–Kontorovich instability arising from the spontaneous emission of acoustic waves at the shock front[54–57]. This instability is also discussed in the experiment by Nilson *et al.* [58] where ultra-high velocity ionizing shocks are generated using Petawatt-class laser pulses. According to our theory, a rather small value of the velocity as small as about 60 km/s produces full ionization and no ultra-high power laser needs to be used. Finally, it is interesting to discuss the effect of the magnetic fields B on ionizing cooling shocks. In the case of radiative cooling, it has been demonstrated that the presence of a weak magnetic field in the ISM ($B \sim 1\,\mu$G) can be compressed up to high values inside the shell of a radiative SNR[59,60]. The tension of magnetic lines tends to decrease the density compression and increase the thickness of the shell. Thus the magnetic field limits the lower value of exponent α and the development of instabilities[61]. The case of ionizing cooling is different. Indeed, the presence of an ambient perpendicular magnetic field B should not affect the present results where the compression at the shock is $\rho_2/\rho_1 = B_2/B_1 \approx (\gamma^*+1)/(\gamma^*-1)$ as long as the Alfven Mach number and the Mach number remain high enough[46,62,63]. This property is also a consequence of the ionizing cooling spatial distribution where all the cooling is localized at the shock front while the radiative cooling is present in the bulk of the plasma with a maximum near the inner boundary of the shell.

ACKNOWLEDGMENTS

A.G. thanks the project Advanced research using high intensity laser produced photons and particles (ADONIS) (CZ.02.1.01/0.0/0.0/16_019/0000789) from European Regional Development Fund.

Appendix A: Reduction of the generalized Rankine-Hugoniot equations

Here, we reduce the three jump equations (2), (3) and (4) to two coupled equations on the new dimensionless unknowns η_2, θ_2 and M defined as,

$$\eta_2 = \frac{\rho_1}{\rho_2}, \qquad \theta_2 = \frac{T_2}{T_1}, \qquad M = \frac{D}{c_1}, \tag{A1}$$

where c_1 is the sound speed in the ambient gas,

$$c_1 = \sqrt{\frac{5P_1}{3\rho_1}} = \sqrt{\frac{5kT_1}{3m_p}}. \tag{A2}$$

Using (2), we find the velocity u_2 in terms of η_2, M and c_1,

$$u_2 = -\eta_2 D = -\eta_2 M c_1. \tag{A3}$$

Then, we inject this relation into (3) and (4) to obtain the two equations,

$$(1+f_2)\theta_2 - \frac{5M^2}{3}(1-\eta_2)\eta_2 - \eta_2 = 0 \tag{A4}$$

$$(1+f_2)\theta_2 - \frac{M^2}{3}(1-{\eta_2}^2) + \frac{2}{5}f_2 a_{ion} - 1 = 0 \tag{A5}$$

where a_{ion} represent the dimensionless ionization energy,

$$a_{ion} = \frac{E_{ion}}{kT_1}. \tag{A6}$$

Then, using (A4), one finds,

$$f_2 = \frac{3+5M^2}{3\theta_2}\eta_2 - \frac{5M^2}{3\theta_2}\eta_2^2 - 1. \tag{A7}$$

By injecting (A7) in (A5), we obtain an equation for the unknown η_2,

$$\begin{aligned} &10M^2(2+\frac{a_{ion}}{\theta_2})\eta_2^2 - (3+5M^2)(5+2\frac{a_{ion}}{\theta_2})\eta_2 \\ &+6a_{ion} + 5(M^2+3) = 0 \end{aligned} \tag{A8}$$

Only one of the two solutions of this second-degree polynomial has a physical meaning and is given by (16).

[1] G. I. Taylor, "Report of civil defense research committee of the ministry of home security," RC-210 **12** (1941).
[2] G. I. Taylor, "The formation of a blast wave by a very intense explosion i. theoretical discussion," Proceedings of the Royal Society of London. Series A. Mathematical and Physical Sciences **201**, 159–174 (1950).
[3] J. von Neumann, "The point source solution"," national defence research committee div. B Report AM-9 (1941).
[4] J. von Neumann and A. Taub, *John von Neumann Collected Works: Volume V-Design of Computers, Theory of Automata and Numerical Analysis* (Pergamon Press, 1963).
[5] L. Sedov, "Propagation of strong shock waves (translated from russian)," Prikl Mat Mekh **10**, 241–250 (1946).

[6]L. Sedov, *Similarity and Dimensional Methods in Mechanics* (CRC Press, 1959).
[7]C. F. McKee and J. P. Ostriker, "A theory of the interstellar medium-three components regulated by supernova explosions in an inhomogeneous substrate," The Astrophysical Journal **218**, 148–169 (1977).
[8]J. P. Ostriker and C. F. McKee, "Astrophysical blastwaves," Reviews of Modern Physics **60**, 1–68 (1988).
[9]R. Bandiera and O. Petruk, "Analytic solutions for the evolution of radiative supernova remnants," Astronomy & Astrophysics **419**, 419–423 (2004).
[10]J. Oort, "Some phenomena connected with interstellar matter (George Darwin lecture)," Monthly Notices of the Royal Astronomical Society **106**, 106–159 (1946).
[11]J. Oort, "Interaction of nova and supernova shells with the interstellar medium," Problems of Cosmical Aerodynamics , 118 (1951).
[12]D. F. Cioffi, C. F. McKee, and E. Bertschinger, "Dynamics of radiative supernova remnants," The Astrophysical Journal **334**, 252–265 (1988).
[13]T. Clayson, S. Lebedev, F. Suzuki-Vidal, G. Burdiak, J. Halliday, J. Hare, J. Ma, L. Suttle, and E. Tubman, "Inverse liner z-pinch: An experimental pulsed power platform for studying radiative shocks," IEEE Transactions on Plasma Science **46**, 3734–3740 (2018).
[14]G. Burdiak, S. Lebedev, R. Drake, A. Harvey-Thompson, G. Swadling, F. Suzuki-Vidal, J. Skidmore, L. Suttle, E. Khoory, L. Pickworth, *et al.*, "The production and evolution of multiple converging radiative shock waves in gas-filled cylindrical liner Z-pinch experiments," High Energy Density Physics **9**, 52–62 (2013).
[15]G. Burdiak, S. Lebedev, F. Suzuki-Vidal, G. Swadling, S. Bland, N. Niasse, L. Suttle, M. Bennet, J. Hare, M. Weinwurm, *et al.*, "Cylindrical liner Z-pinch experiments for fusion research and high-energy-density physics," Journal of Plasma Physics **81**, 365810301 (2015).
[16]J. Grun, J. Stamper, C. Manka, J. Resnick, R. Burris, J. Crawford, and B. Ripin, "Instability of Taylor-Sedov blast waves propagating through a uniform gas," Physical Review Letters **66**, 2738–2741 (1991).
[17]M. Edwards, A. MacKinnon, J. Zweiback, K. Shigemori, D. Ryutov, A. Rubenchik, K. Keilty, E. Liang, B. Remington, and T. Ditmire, "Investigation of ultrafast laser-driven radiative blast waves," Physical Review Letters **87**, 085004 (2001).
[18]A. Edens, R. G. Adams, P. Rambo, L. Ruggles, I. C. Smith, J. L. Porter, and T. Ditmire, "Study of high mach number laser driven blast waves in gases," Physics of Plasmas **17**, 112104 (2010).
[19]D. Symes, M. Hohenberger, J. Lazarus, J. Osterhoff, A. Moore, R. Fäustlin, A. Edens, H. Doyle, R. Carley, A. Marocchino, *et al.*, "Investigations of laser-driven radiative blast waves in clustered gases," High Energy Density Physics **6**, 274–279 (2010).
[20]N. Riley, S. Lewis, M. Wisher, M. Kimmel, K. Struve, J. Porter, R. Bengtson, and T. Ditmire, "Improved experimental resolution of the Vishniac overstability in scaled late-stage supernova remnants," High Energy Density Physics **22**, 64–72 (2017).
[21]A. Edens, T. Ditmire, J. Hansen, M. Edwards, R. Adams, P. Rambo, L. Ruggles, I. Smith, and J. Porter, "Study of high mach number laser driven blast waves," Physics of Plasmas **11**, 4968–4972 (2004).
[22]A. Reighard, R. P. Drake, K. Dannenberg, D. Kremer, M. Grosskopf, E. C. Harding, D. Leibrandt, S. G. Glendinning, T. Perry, B. A. Remington, *et al.*, "Observation of collapsing radiative shocks in laboratory experiments," Physics of Plasmas **13**, 082901 (2006).
[23]R. Sachs, "Some properties of very intense shock waves," Physical Review **69**, 514–522 (1946).
[24]C. Michaut, C. Stehlé, S. Leygnac, T. Lanz, and L. Boireau, "Jump conditions in hypersonic shocks," The European Physical Journal D-Atomic, Molecular, Optical and Plasma Physics **28**, 381–392 (2004).
[25]C. A. Whitney and A. J. Skalafuris, "The structure of a shock front in atomic hydrogen. I: The effects of precursor radiation in the Lyman continuum." The Astrophysical Journal **138**, 200 (1963).
[26]A. J. Skalafuris, "The structure of a shock front in atomic hydrogen. II: The region of internal relaxation." The Astrophysical Journal **142**, 351 (1965).
[27]A. J. Skalafuris, "The structure of a shock front in atomic hydrogen. III: The radiative relaxation region," Astrophysics and Space Science **2**, 258–278 (1968).
[28]A. J. Skalafuris, "The structure of a shock front in atomic hydrogen. IV: Stability, dissipation, and propagation," Astrophysics and Space Science **3**, 234–257 (1969).
[29]H. Nieuwenhuijzen, C. De Jager, M. Cuntz, A. Lobel, and L. Achmad, "A generalized version of the Rankine-Hugoniot relations including ionization, dissociation and related phenomena," Astronomy and Astrophysics **280**, 195–200 (1993).
[30]A. Robinson and J. Pasley, "Potential for the Vishniac instability in ionizing shock waves propagating into cold gases," Physics of Plasmas **25**, 052701 (2018).
[31]D. Domínguez-Vázquez and R. Fernandez-Feria, "On analytical approximations for the structure of a shock wave in a fully ionized plasma," Physics of Plasmas **26**, 082118 (2019).
[32]G. I. Barenblatt, *Scaling, self-similarity, and intermediate asymptotics: dimensional analysis and intermediate asymptotics*, 14 (Cambridge University Press, 1996).
[33]Y. B. Zel'Dovich and Y. P. Raizer, *Physics of shock waves and high-temperature hydrodynamic phenomena* (Courier Corporation, 2002).
[34]D. D. Clayton, *Principles of stellar evolution and nucleosynthesis* (University of Chicago press, 1983).
[35]J. D. Hey, C. Chu, and J. Rash, "Partial local thermal equilibrium in a low-temperature hydrogen plasma," Journal of Quantitative Spectroscopy and Radiative Transfer **62**, 371–387 (1999).
[36]G. Barenblatt and G. Sivashinskii, "Self-similar solutions of the second kind in the problem of propagation of intense shock waves," Journal of Applied Mathematics and Mechanics **34**, 655–662 (1970).
[37]A. Preite-Martinez, "Late-stage evolution of a supernova remnant-The structure of the dense shell," Astronomy and Astrophysics **96**, 283–292 (1981).
[38]J. M. Blondin, E. B. Wright, K. J. Borkowski, and S. P. Reynolds, "Transition to the radiative phase in supernova remnants," The Astrophysical Journal **500**, 342 (1998).
[39]D. Badjin, S. Glazyrin, K. Manukovskiy, and S. Blinnikov, "On physical and numerical instabilities arising in simulations of non-stationary radiatively cooling shocks," Monthly Notices of the Royal Astronomical Society **459**, 2188–2211 (2016).
[40]J. Minière, S. Bouquet, C. Michaut, J. Sanz, and M. Mancini, "Numerical study of the vishniac instability in cooled supernova remnants," Astronomy & Astrophysics **617**, A133 (2018).
[41]S. Falle, "Numerical calculation of thin shell formation in supernova remnants," Monthly Notices of the Royal Astronomical Society **172**, 55–84 (1975).
[42]S. Falle, "Catastrophic cooling in supernova remnants," Monthly Notices of the Royal Astronomical Society **195**, 1011–1028 (1981).
[43]R. A. Chevalier, "The evolution of supernova remnants. Spherically symmetric models," The Astrophysical Journal **188**, 501–516 (1974).
[44]W. Straka, "Numerical models of the evolution of supernova remnants: the shell-formation stage," The Astrophysical Journal **190**, 59–66 (1974).
[45]L. D. Landau and E. M. Lifshitz, *Fluid Mechanics: Course of Theoretical Physics*, Vol. 6 (Elsevier, 2013).
[46]R. P. Drake, *High-energy-density physics: foundation of inertial fusion and experimental astrophysics* (Springer, 2018).
[47]V. Andrushchenko, G. Barenblatt, and L. Chudov, "Self-similar propagation of strong blast waves in the presence of radiation or energy release at the wave front," Collection of papers dedicated to the 100th anniversary of B.G. Galerkin, Shapiro, G.S. (ed.), (in Russian) Nauka, Moscow , 35–44 (1975).
[48]A. Gintrand, J. Sanz, S. Bouquet, and J. Paradela, "Self-similar dynamics of radiative blast waves," Physics of Fluids **32**, 016105 (2020).
[49]A. Gintrand, Q. Moreno-Gelos, A. Araudo, V. Tikhonchuk, and S. Weber, "Collision between radiative and adiabatic supersonic flows," The Astrophysical Journal **920**, 113 (2021).
[50]E. T. Vishniac, "The dynamic and gravitational instabilities of spherical shocks," The Astrophysical Journal **274**, 152–167 (1983).
[51]D. Ryu and E. T. Vishniac, "The Growth of Linear Perturbations of Adiabatic Shock Waves," The Astrophysical Journal **313**, 820 (1987).
[52]J. Sanz, S. Bouquet, C. Michaut, and J. Miniere, "The spectrum of the Sedov–Taylor point explosion linear stability," Physics of Plasmas **23**, 062114 (2016).
[53]C. Michaut, C. Cavet, S. Bouquet, F. Roy, and H. Nguyen, "Numerical study of the vishniac instability in supernova remnants," The Astrophysical Journal **759**, 78 (2012).
[54]S. D'yakov, "Shock wave stability," Zh. Eksp. Teor. Fiz **27**, 288–295 (1954).

[55]V. Kontorovich, "On the shock waves stability," Zh. Eksp. Teor. Fiz **33**, 1525–1526 (1957).
[56]J. W. Bates and D. C. Montgomery, "The D'yakov-Kontorovich instability of shock waves in real gases," Physical Review Letters **84**, 1180–1183 (2000).
[57]C. Huete, F. Cobos-Campos, E. Abdikamalov, and S. Bouquet, "Acoustic stability of nonadiabatic high-energy-density shocks," Physical Review Fluids **5**, 113403 (2020).
[58]P. Nilson, S. Mangles, L. Willingale, M. Kaluza, A. Thomas, M. Tatarakis, Z. Najmudin, R. Clarke, K. Lancaster, S. Karsch, *et al.*, "Generation of ultrahigh-velocity ionizing shocks with petawatt-class laser pulses," Physical Review Letters **103**, 255001 (2009).
[59]O. Petruk, T. Kuzyo, and V. Beshley, "Post-adiabatic supernova remnants in an interstellar magnetic field: parallel and perpendicular shocks," Monthly Notices of the Royal Astronomical Society **456**, 2343–2353 (2015).
[60]O. Petruk, T. Kuzyo, S. Orlando, M. Pohl, M. Miceli, F. Bocchino, V. Beshley, and R. Brose, "Post-adiabatic supernova remnants in an interstellar magnetic field: oblique shocks and non-uniform environment," Monthly Notices of the Royal Astronomical Society **479**, 4253–4270 (2018).
[61]D. A. Badjin and S. I. Glazyrin, "Physical and numerical instabilities of radiatively cooling shocks in turbulent magnetized media," Monthly Notices of the Royal Astronomical Society **507**, 1492–1512 (2021).
[62]J. P. Goedbloed, R. Keppens, and S. Poedts, *Advanced magnetohydrodynamics: with applications to laboratory and astrophysical plasmas* (Cambridge University Press, 2010).
[63]S. Galtier, *Introduction to modern magnetohydrodynamics* (Cambridge University Press, 2016).